Available online at www.sciencedirect.com

ScienceDirect

Procedia – Social and Behavioral Sciences (2011) 000–000

Procedia Social and Behavioral Sciences

www.elsevier.com/locate/procedia

The 19th International Symposium on Transportation and Traffic Theory

Freeway Traffic Oscillations: Microscopic Analysis of Formations and Propagations using Wavelet Transform

Zuduo Zheng[a], Soyoung Ahn[a]1*, Danjue Chen[b], Jorge Laval[b]

[a]*Arizona State University, P.O. Box 875306,Tempe, AZ 85287, U.S.A.*
[b]*Georgia Institute of Technology,790 Atlantic Dr. Atlanta, GA 30332-0355, U.S.A.*

Abstract

In this paper we identify the origins of stop-and-go (or slow-and-go) driving and measure microscopic features of their propagations by analyzing vehicle trajectories via Wavelet Transform. Based on 53 oscillation cases analyzed, we find that oscillations can be originated by either lane-changing maneuvers (LCMs) or car-following behavior (CF). LCMs were predominantly responsible for oscillation formations in the absence of considerable horizontal or vertical curves, whereas oscillations formed spontaneously near roadside work on an uphill segment. Regardless of the trigger, the features of oscillation propagations were similar in terms of propagation speed, oscillation duration, and amplitude. All observed cases initially exhibited a precursor phase, in which slow-and-go motions were localized. Some of them eventually transitioned into a well-developed phase, in which oscillations propagated upstream in queue. LCMs were primarily responsible for the transition, although some transitions occurred without LCMs. Our findings also suggest that an oscillation has a regressive effect on car-following behavior: a deceleration wave of an oscillation affects a timid driver (characterized by larger response time and/or minimum spacing) to become less timid and an aggressive driver less aggressive, although this change may be short-lived. An extended framework of Newell's CF model is able to describe the regressive effects with two additional parameters with reasonable accuracy, as verified using vehicle trajectory data.

Keywords: Car-following behavior; Lane-changing maneuver; Stop-and-go traffic; Traffic oscillations; Wavelet Transform

* Corresponding author. Tel.: +1-480-965-1052; fax: +1480-965-0557.
E-mail address: sue.ahn@asu.edu.

1. Introduction

Traffic oscillations refer to the stop-and-go driving conditions in congested traffic that cause drivers to exhibit oscillatory trajectories with regular deceleration/acceleration cycles. These disturbances typically form near active freeway bottlenecks (Ahn & Cassidy, 2007) and propagate against traffic flow at relatively constant speeds of 10-20 km/hr without fanning out (Mauch & Cassidy, 2002; Ahn, 2005; Lu & Skabardonis, 2007; Schonhof & Helbing, 2007). They often grow in amplitude as they propagate (Mauch & Cassidy, 2002) and adversely impact traffic safety (Zheng, Ahn & Monsere, 2010).

Traditional wisdom indicates that traffic oscillations are induced by instabilities in longitudinal vehicle interactions (e.g., Herman, Motroll & Potts, 1959). In support of this premise, oscillations were observed on a single-lane facility (Smilowitz, Daganzo, Cassidy, & Bertini, 1999), a test-track (Sugiyama et al., 2003) and a tunnel where lane-changing maneuvers (LCMs) were prohibited (Edie and Baverez, 1958). Other studies (Kerner & Rehborn, 1996, Mauch & Cassidy, 2002; Ahn & Cassidy, 2007) provide empirical evidence that LCMs are primarily responsible for oscillations' formations and growths on multilane freeways. In particular, Ahn and Cassidy (2007) analyzed several instances of formations and growths using trajectory data and confirmed that LCMs are indeed a primary factor. However, they also observed that oscillations often grew in amplitude without LCM. Laval and Leclercq (2010) showed that the growth without LCM is attributed to driver characteristics (timid vs. aggressive).

Several car-following (CF) models have recently been proposed to replicate oscillations by assuming probabilistic headways during decelerations (Del Castillo, 2001) or probabilistic reaction time (Kim & Zhang, 2008). In addition to the free-flow and congested regimes, Orosz, Wilson, Szalai, and Stépán (2009) defined a third regime, called the "excitable regime." Traffic flow in this regime is stable but sensitive to external perturbations, which leads to oscillations' formations. Yeo and Skabardonis (2010) proposed an asymmetric traffic theory in which five traffic states are defined: acceleration, deceleration, coasting, stationary, and free flow. During a coasting state, a vehicle changes its spacing at a constant speed. Other states are self-explanatory. In their conjecture, stop-and-go waves generate near a deceleration curve in congested traffic. The waves propagate upstream (or dissipate) if the following traffic is near the deceleration (acceleration) curve. They have tested their theory by plotting and visually checking trajectory data. Laval and Leclercq (2010) criticized the lack of physical meaning of these models and proposed an extended framework of Newell's CF theory (Newell, 2002) to incorporate different driver characteristics.

Despite numerous studies on oscillations, our understanding of oscillations is not sufficient. Most existing studies were conducted using loop detector data, whose resolution is not adequate to reveal the mechanism of oscillations. Sugiyama et al. (2003) and Ahn and Cassidy (2007) are among the first studies to explicitly show that oscillations can be triggered by either car-following or lane-changing. However, these studies were conducted in a controlled environment (a circular track in Sugiyama et al., 2003) or using a small sample of vehicle trajectory data on a single location (Ahn and Cassidy, 2007). Moreover, trajectory data are noisy due to wide variations in driver behavior. Thus, analyzing the trajectory data in a systematic and reproducible way has been challenging, and subjective judgment was often applied in interpreting the data. Finally, existing (microscopic) models are often calibrated and validated using simulations, macroscopic data (i.e., loop detector data), or limited trajectory data. This is due to the fact that there is lack of systematic methods to analyze oscillations at the individual vehicle level.

In this paper we address the shortcomings of previous studies and identify oscillations' triggers at the vehicle level and analyze the propagation features in a comprehensive and systematic manner using Wavelet Transform (WT). Zheng, Ahn, Chen, and Laval (2011a) demonstrate using small samples that WT is effective for analyzing bottleneck activations, regime transitions, and traffic oscillations. In view of this, we adopt WT to analyze a large number of oscillations (53 cases) in a systematic and efficient way, while minimizing subjective judgment in data processing. Our findings elucidate to what extent LCMs or instabilities in CF are responsible for formations. We also investigate propagation characteristics for different triggers, including the transition mechanism from precursor to well-developed phases of oscillations. Finally, this study investigates the impact of oscillations on driver behavior.

The remainder of this paper is organized as follows. Section 2 presents a summary of the theoretical background of WT and its adaptation to analyze traffic data. Section 3 describes the study sites and data. Section 4 discusses findings related to oscillations' formations. Section 5 describes the characteristics (i.e., duration, amplitude, and

intensity) of oscillations along their propagation paths and the effects of LCMs and CF behavior. Finally, conclusions and future research are summarized in Section 6.

2. Background: Wavelet Transform (WT)

As we note in the previous section, existing methods have limitations in analyzing oscillations in ways that are efficient, objective, and reproducible. Li, Peng, and Ouyang (2010) and Zheng et al. (2011a) provide comprehensive reviews on existing techniques. Zheng et al. (2011a) describe the mathematical theory of WT and demonstrate its potential applications for analyzing various features of congested traffic including bottleneck activations, regime transitions, and traffic oscillations. Here, we adopt this method to analyze oscillations in depth. A summary of WT described in Zheng et al. (2011a) follows.

As a time-frequency decomposition tool, WT is effective in extracting local information from non-stationary time series because in the wavelet framework, any local changes can be captured by moving the wavelet along the time domain and changing the scale (i.e., squeezing or dilating the wavelet). With such time-scale representation of a noisy and aperiodic time series data (e.g., oscillatory traffic data), WT can preserve underlying features while removing trivial events.

A wavelet is a (real or complex) mathematical function, $\psi(t)$, that transforms continuous time series data into various scale components. The Mexican hat wavelet, as defined in (1), is selected in this study because of its similar shape to a typical cycle of traffic oscillation and small Shannon entropy (Addison, 2002; Fugal, 2009).

$$\psi\left(\frac{t-b}{a}\right) = \left[1 - \left(\frac{t-b}{a}\right)^2\right] e^{-\frac{\left(\frac{t-b}{a}\right)^2}{2}} \qquad (1)$$

where a is a scale parameter that governs the dilation and contraction of the wavelet, and b is a translation parameter that governs the movement of the wavelet along the time dimension. Note from (1) that the Mexican hat mother wavelet ($a = 1$ and $b = 0$) is the second derivative of Gaussian distribution function, $e^{-\frac{t^2}{2}}$.

For our analysis, time series speed of a vehicle, $v(t)$, is a continuous signal function. A WT coefficient of $v(t)$ is

$$T(a,b) = w(a) \int_{-\infty}^{\infty} v(t) \left[1 - \left(\frac{t-b}{a}\right)^2\right] e^{-\frac{\left(\frac{t-b}{a}\right)^2}{2}} dt \qquad (2)$$

where $w(a)$ is a weighting function and typically set to $1/\sqrt{a}$ to ensure that the wavelets at all scales have the same energy. $T(a, b)$ is a transformed signal at location b and scale a in the wavelet dimension. Then, the average wavelet-based energy at b is computed based on the WT coefficients for different scales, as defined in equation (3).

$$E_b = \frac{1}{\max(a)} \int_0^{\max(a)} |T(a,b)|^2 da \qquad (3)$$

where max (a) represents the maximum scale, which is set to avoid potential distortion of the overall energy due to large scale trends (see Zheng et al. (2011a) for details). An abrupt speed change in time generates a sharp peak in temporal distribution of wavelet-based energy. As demonstrated hereafter, this property is used to identify vehicles that initiate disturbances and trace oscillation waves that accompany sudden decelerations or accelerations.

3. Sites and Data

For this study, we analyzed the vehicle trajectory data collected by FHWA's Next Generation Simulation (NGSIM) program (FHWA, 2008). Study sites consist of a 1650-ft section on northbound I-80 in Emeryville, California (Figure 1(a)) and a 2100-ft section on southbound US-101 in Los Angeles, California (Figure 1(b)). At each site, the trajectory data were collected for 45 min near or under congestion with 0.1-sec resolution. These high resolution trajectory data are ideal for a microscopic investigation of formation and propagation of oscillations. For our analysis, we exclude 1) the LCMs that lasted less than 5 sec because they are likely noises (Thiemann, Treiber,

& Kesting, 2008), 2) the HOV lane (Lane 1) at I-80 because driving behavior in the HOV lane might be different from that in regular-use lanes.

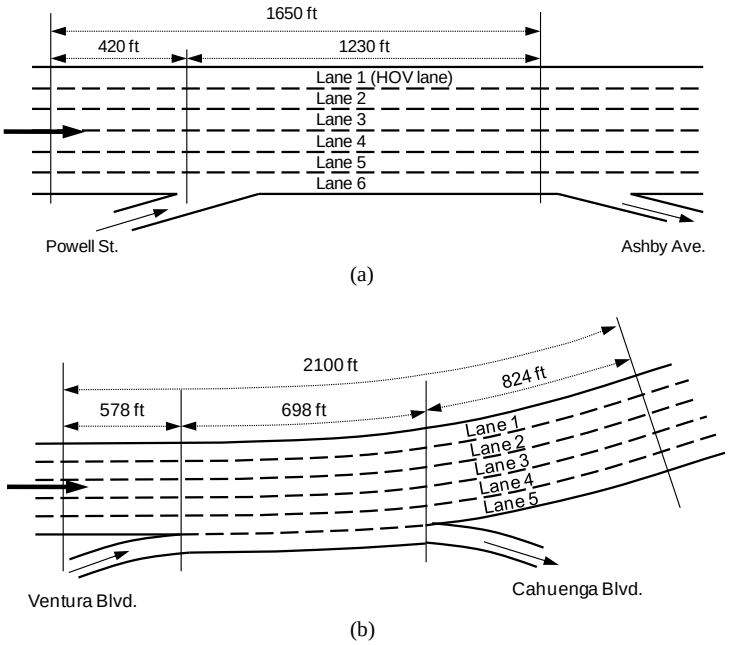

Figure 1 Schematic illustration of study sites; (a) northbound I-80 in Emeryville, California; (b) southbound US-101 in Los Angeles, California; Lane numbering is incremented from the left-most lane.

4. Formations of Traffic Oscillations

This section describes the ways in which we identified oscillation formations and their causes. We define an oscillation as a deceleration phase followed by an acceleration phase. Thus, approximate times and locations of oscillation formations can be identified using speed contours. For instance, Figure 2 shows a speed contour plot constructed for lane 1 (median lane) on US-101 by aggregating the trajectory data with resolution of 50 ft by 5 sec. Each time-space region is shaded based on the corresponding mean speed according to the gray scale shown in the legend. The dark regions correspond to states with low speeds. The figure clearly reveals several instances of oscillation formations (with periods of about 2 minutes) near location 1500 ft and their orderly propagations against traffic flow. We identified 53 cases of oscillation formations across all lanes and sites.

For each oscillation case, we use temporal distributions of wavelet-based energy for individual vehicles to trace the origin, more precisely the vehicle that initiated a deceleration state. The maximum scale is set at 64 (6.4 s in the time domain since the time resolution is 0.1 sec) to ensure that a wavelet window does not include more than one deceleration or acceleration phase (Zheng et al., 2011a; Mallat, 2009). Any speed change due to a sudden deceleration or acceleration is translated to a spike in the temporal energy distribution. Thus, the origin of an oscillation can be traced by identifying the first vehicle that displays a noticeable energy spike. For instance, Figure 3(a) shows vehicle trajectories on lane 1, US-101, which display formation and propagation of a noticeable oscillation. We magnify a subset of these trajectories (Figure 3(b)) to better isolate the origin; however, the origin of the deceleration wave is still not apparent to naked eye and debatable between vehicle 2 (a lane-changer) and vehicle 39. The wavelet-based energy distributions in Figure 3(c) reveal that vehicle 2 did not cause the deceleration wave. (Note that each energy distribution is separated vertically by adding a constant to reveal a spatial pattern of energy peaks.) The energy peaks displayed by the lane-changer reflect speed changes during maneuvering; however, these speed changes were isolated to the lane-changer and did not affect the following vehicles (vehicles 10-27). Another

noticeable energy peaks appeared with vehicle 39 and propagated to following vehicles 43 and 54. Thus, we conclude that this deceleration wave was triggered by the car-following behavior of vehicle 39.

In contrast, for the case shown in Figure 4(a), the origin can be traced back to a lane-changer. The wavelet-based energy in Figure 4(b) reveals that the first perceptible energy peaks occurred with vehicle 2389, a follower of two lane-changers, vehicles 2376 and 2384. These energy peaks propagated to the following vehicles upstream. Therefore, this oscillation was apparently triggered by the LCMs.

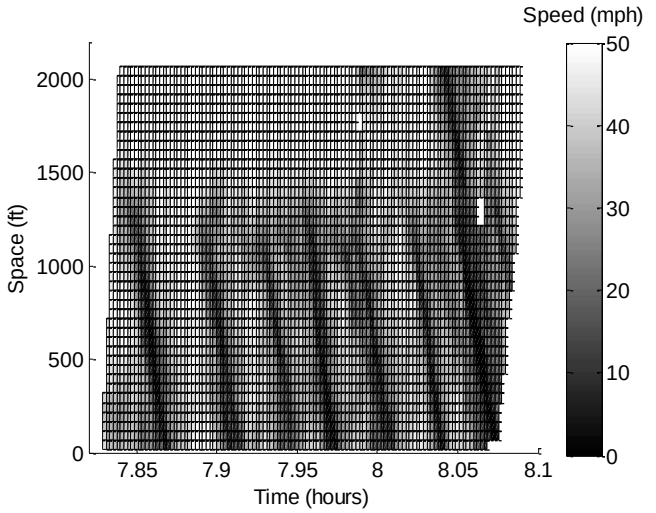

Figure 2 Speed contour for lane 1, US 101.

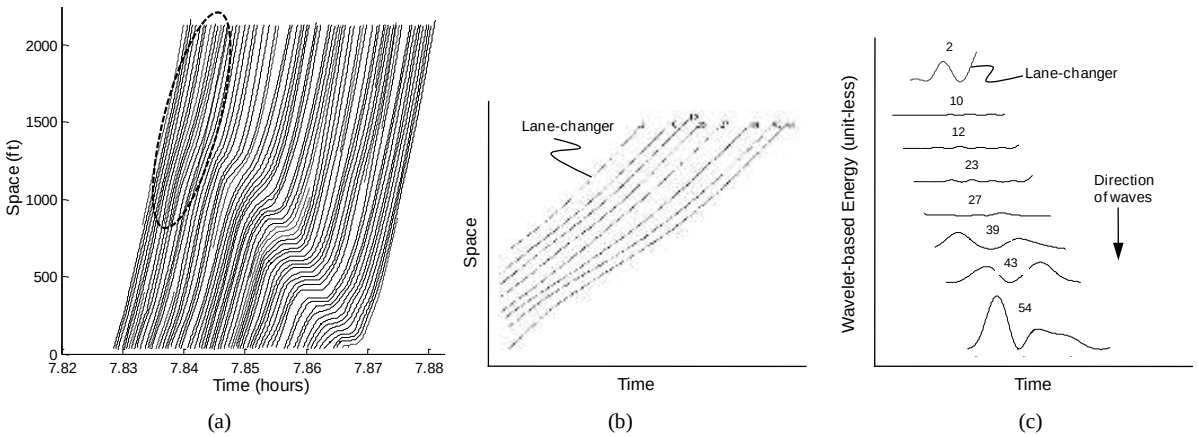

Figure 3 Example of identifying oscillation formation (lane 1, US-101) (a) Vehicle trajectories displaying a noticeable oscillation; (b) Vehicle trajectories near the origin of the oscillation; (c) Temporal distributions of wavelet-based energy for the vehicles near the oscillation's origin; The energy distribution for each vehicle is separated with a vertical displacement to better display the propagation of energy peaks.

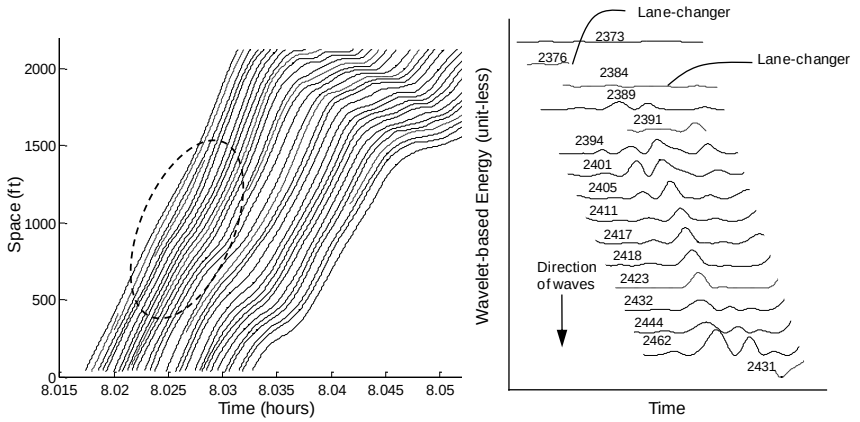

(a) (b)

Figure 4 Example of identifying oscillation formation (lane 1, US-101) (a) Vehicle trajectories displaying a noticeable oscillation; (b) Temporal distributions of wavelet-based energy for the vehicles near the oscillation's origin; The energy distribution for each vehicle is separated with a vertical displacement to better display the propagation of energy peaks.

The analysis results from all 53 formation cases are summarized in Table 1. On 1-80, the majority of the cases were originated by LCMs rather than instabilities in driver behavior (16 vs. 2 cases). In contrast, approximately 66% of the cases were originated by instabilities in driver behavior on US-101. The results suggest that oscillations can be instigated by different factors and that the predominant trigger is site-specific. Notably, the study site on I-80 is a relatively straight segment on a level terrain but features multiple merges (a freeway merge, an on-ramp, and a lane-reduction) and a diverge within or nearby the study section. Thus, the effect of geometric alignment is presumably minimal, but many LCMs are expected. In contrast, the US-101 site is on an uphill segment and includes a merge and a diverge within the study site. Moreover, video footage of the study site shows some maintenance activity in the median during the data collection period. Besides the distraction, the uphill segment is likely to accentuate differences in vehicle characteristics, such as acceleration capability, which may instigate oscillations spontaneously without LCMs.

Table 1 Summary of the oscillations' triggers

	Lane-changing	Non-lane-changing	Total
US-101	12	23	35
I-80	16	2	18
Total	28	25	53

5. Propagations of Traffic Oscillations

In the previous section, we showed that oscillations can be instigated by different factors. Here, we investigate how these oscillations propagate in space and if different causal factors lead to distinct patterns of oscillation propagations.

5.1. The effect of oscillation triggers on propagation features

To study the propagation features of oscillations, we first trace the propagation paths of deceleration and acceleration waves through vehicles using WT. The arrival of a (deceleration or acceleration) wave is marked by an

energy peak in the temporal energy distribution (characteristic point hereafter). Thus, the propagation of an oscillation is identified by tracing the energy peaks between vehicles.

Figure 5(a) shows the propagation of the oscillation shown in Figure 3. The first propagation path marks the passage of a deceleration wave, which is followed by another path marking an acceleration wave. Note that these paths correspond to the starting points of decelerations and accelerations (indicating wave arrivals), rather than peaks as one might identify visually from trajectories. The spatiotemporal development of this deceleration state initially exhibits a precursor phase, during which speed changes of vehicles are rather moderate, and the waves propagate with nearly zero speed (i.e., the oscillation in the precursor period propagates from vehicle to vehicle, but not in space). Emerging from the precursor period, the oscillation becomes more developed with larger speed changes and propagates backward in space in a more stable manner. (The existence of a precursor phase is also demonstrated in Laval and Leclercq (2010).) Of note, the precursor and the subsequent phases are distinguished using the Bottom-Up algorithm. It searches a break point that minimizes mean-squared-error of linear regressions in the two phases. The average wave speed in the identified precursor state is close to zero (< 1 mph).

Note that the slope of each path represents the wave propagation speed. The estimated average speed (after the precursor period) via regression is 11.8 ft/s (8 mph) for the deceleration wave (R^2=0.96) and 17 ft/s (11.6 mph) for the acceleration wave (R^2=0.98). Based on the wave propagation paths, we measure the amplitude, duration, and intensity of each vehicle in a deceleration state. Figure 5(b) presents the oscillation duration for each vehicle, which is estimated as the duration between two characteristics points. The figure reveals that the duration of the deceleration state increases slightly for the first 31 vehicles and then decreases, with an average of about 16 seconds. A similar trend is observed for the amplitude (see Figure 5(c)), which is measured as the speed difference between the first and the second characteristics points. However, the intensity in Figure 5(d), which is defined as amplitude/duration to measure the rate of speed decrease, displays a relatively stable trend.

Independent of the trigger, all 53 oscillations exhibited a precursor phase. Of 53 oscillations, 22 eventually emerged from the precursor phase and became well-developed. For the 22 well-developed oscillations, the propagation speed, duration, and amplitude are summarized by the trigger in Table 2. It shows that 1) the propagation speed and duration are consistent throughout the 22 cases; and 2) the propagation characteristics are similar between oscillations with two different triggers. 2) is confirmed statistically: assuming that wave propagation speed is normally distributed, the differences between the two groups of oscillations are not significant at the 95% confidence level. Findings suggest that oscillations propagate in a similar manner independent of the trigger.

Table 2 Propagation speed, amplitude and duration of oscillations triggered by CF or LCM

Oscillations triggered by CF				Oscillations triggered by LCM			
ID	Propagation Speed (ft/s)	Amplitude (ft/s)	Duration (sec)	ID	Propagation Speed (ft/s)	Amplitude (ft/s)	Duration (sec)
1	17.54	52.06	10.75	13	14.26	37.83	11.34
2	12.75	30.86	10.21	14	14.97	29.08	7.023
3	14.91	52.52	16.90	15	15.63	36.28	11.58
4	14.63	47.19	12.90	16	13.71	30.62	12.69
5	17.59	53.05	11.26	17	12.58	27.94	8.06
6	15.15	41.66	11.07	18	14.95	30.02	8.09
7	15.90	41.20	14.94	19	17.55	46.18	13.82
8	15.12	28.52	9.45	20	17.21	21.20	8
9	13.78	28.54	14.55	21	16.20	32.48	9.65
10	15.61	22.56	11.45	22	16.54	28.93	11.85
11	13.48	31.09	9.81	Mean	15.36	32.06	10.21
12	12	31.33	14.58	Std. Error	0.456	1.951	0.678
Mean	14.87	38.38	12.32				
Std. Error	0.494	3.141	0.693				

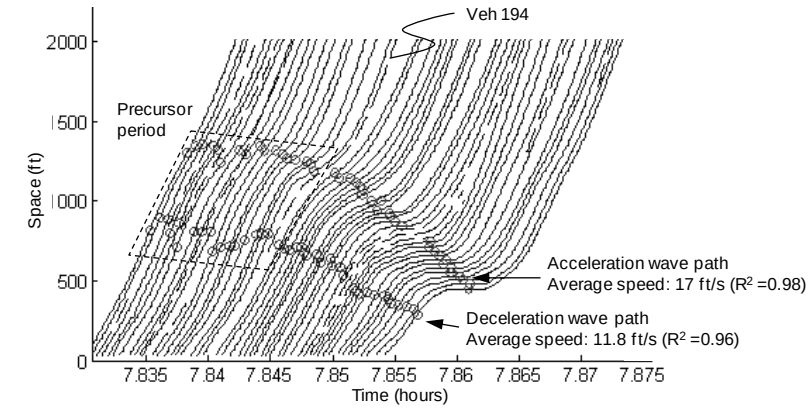

(a)

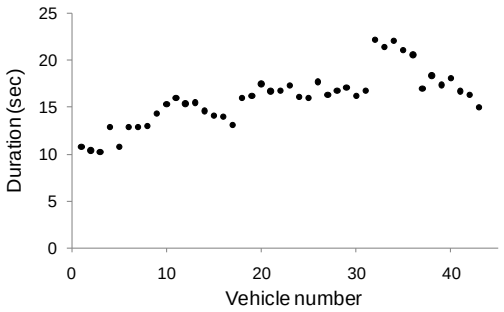

(b)

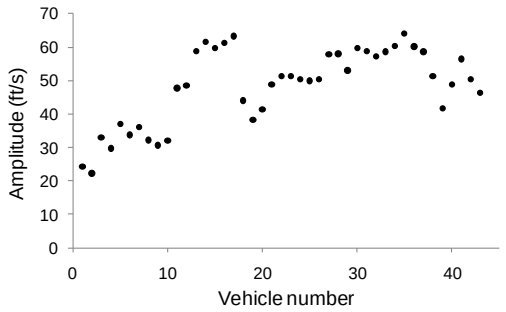

(c)

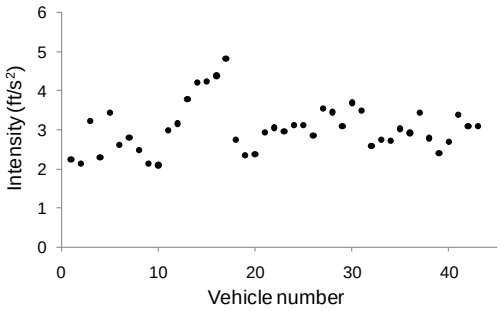

(d)

Figure 5 Example of the propagation of a decelerated state (lane 1, US-101); (a) the wave propagation paths; (b) the duration of the decelerated state; (c) the amplitude of the decelerated state; (d) the intensity of the decelerated state.

5.2. The effects of LCMs on oscillation propagation

Here we demonstrate that LCMs are primarily responsible for the transition from a precursor to a well-developed phase. For example, a closer inspection of Figure 5 reveals that the precursor phase ended with the insertion of vehicle 194, and the oscillation started to propagate backward in space with increasing amplitudes. Similar examples are shown in Figure 6, which present several cycles of oscillations. The deceleration state bounded by waves 1 and 2 (denoted as *w1* and *w2* in the figure) initially underwent a precursor phase and then became well-developed after the insertion of vehicle 313. This same lane-changer also ended the precursor phase of the deceleration state bounded by waves 3 and 4. For 15 cases out of 22, transition into the well-developed phase was attributable to LCM (more precisely, vehicle insertions), though transition also occurred without LCM in 7 cases.

Figure 6 also uncovers other interesting effects of LCMs. The deceleration state bounded by waves 5 and 6 propagated at speed of approximately 9 mph before the insertion of vehicle 313. The propagation speed then increased to about 14 mph after the insertion, indicating that LCMs may alter the propagation speed. In contrast, an exit maneuver may dampen oscillations. The decelerated state marked by waves 7 and 8, for example, disappeared (or returned to a precursor phase) with the exit of vehicle 219. The disappearance was short-lived, however, as another deceleration state (bounded by waves 3 and 4) emerged a few vehicles upstream. The above observations underline the importance of LCMs' impact in traffic stream and warrant a more systematic investigation of LCMs. Zheng, Ahn, Chen, and Laval (2011b) offer some insights on this issue.

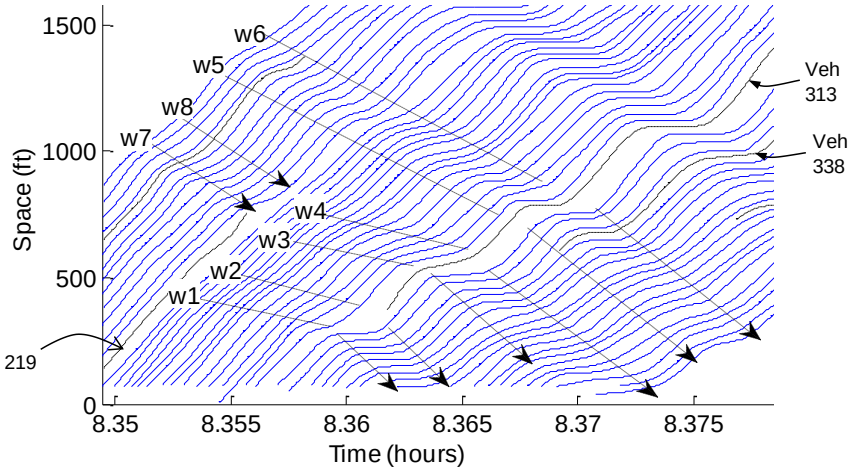

Figure 6 Illustration of LCM's impacts on oscillation's propagation on the basis of vehicle trajectories; a dashed line is a lane changer's trajectory; a solid line is a non-lane-changer's trajectory; a dotted line traces a wave propagation.

5.3. Regressive effect of oscillations on CF behavior

This section describes the change in CF behavior when a driver crosses a deceleration wave, which results in a change in deceleration duration. We explain this change in CF behavior based on Newell's CF theory (Newell, 2002) and offer an extended framework to capture the change as we describe hereafter.

Newell (2002) postulated that on a homogenous highway the trajectory of a vehicle ($x_n(t)$ in Figure 7) in congested traffic is identical to the preceding vehicle's trajectory ($x_{n-1}(t)$ in Figure 7) except for shifts in space, d_n, and time, τ_n . Thus, τ_n represents response time, the duration that vehicle n waits until it changes its speed in response to the leader's change in speed, and d_n represents the minimum (jam) spacing. Newell further conjectured that (τ_n, d_n) vary between vehicles due to driver differences but are constant independent of speed for each driver. Then spacing of vehicle n, s_n, solely depends on speed, v: i.e,

$$s_n = d_n + \tau_n v. \qquad (4)$$

Newell's CF model is notable for its consistency with simplified kinematic wave theory (Newell, 1993).

In this study, two sets of τ and d are measured for each vehicle; (τ_1 and d_1) and (τ_2 and d_2) based on the first and the second characteristics points, respectively, marking the arrivals of a deceleration followed by an acceleration waves. If Newell's theory holds, (τ_1 and d_1) and (τ_2 and d_2) should be the same for each vehicle, and the deceleration duration should be constant across vehicles. Interestingly, we found that the deceleration duration, u, changes between vehicles and is significantly related to τ_1 and d_1. More specifically, Figure 8 shows τ_1 vs. u for the 489 vehicles involved in the 22 well-developed oscillations. A large variation in τ is observed, though the majority of τ lie between 0 and 5 sec. The figure also reveals a negative relationship between τ and u, which is significant at the 99% confidence level, despite the noticeable variations. Thus, a vehicle with a larger value of τ exhibits shorter deceleration duration. This observation implies that unlike Newell's premise, τ can change for a vehicle, especially when it goes through a major speed disturbance.

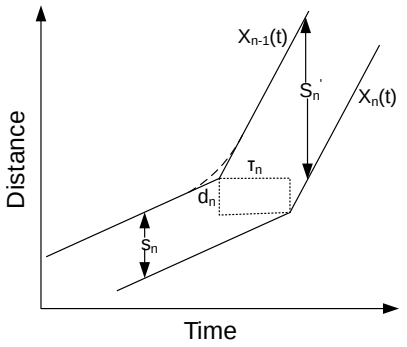

Figure 7 Piecewise linear approximation to vehicle trajectories (Adopted from Newell (2002))

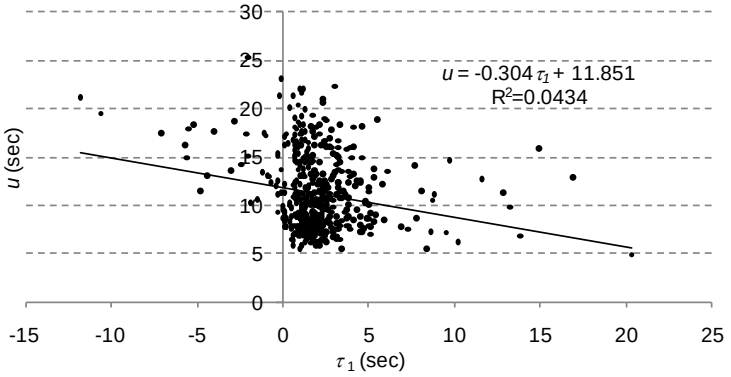

Figure 8 Relationship between τ_1 and deceleration duration, u

Based on the above finding, we predict the amount of change in τ due to oscillations and extend Newell's model. Notably, Zheng et al. (2011b) studied the impact of a lane-changing maneuver by analyzing anticipation and relaxation processes of the follower in the target lane and a change in the follower's behavior induced by the maneuver. The change in behavior is measured by comparing τ and d before and after the maneuver using Newell's CF model. They found that a LCM has a regressive effect on driver CF behavior: a timid driver with larger response time (τ) and/or minimum spacing (d) tends to become less timid and an aggressive driver less aggressive after a LCM. The extent of a behavioral change depends on the amount of deviation from the "average" driving behavior before experiencing a LCM. We postulate that an oscillation, more precisely a deceleration wave, has a similar effect.

In testing the regressive effect of a deceleration wave, we consider the following linear framework as in Zheng et al. (2011b) to keep the model parsimonious:

$$\tau_2 - \tau_1 = \alpha(\tau_1 - \bar{\tau}) + \beta, \qquad (5)$$

where $\bar{\tau}$ and $\bar{d}$ are the average τ_1 and d_1 (1.98 sec and 24.61 ft, respectively) and assumed to represent *average* driving behavior. To cross-validate our model, we (randomly) divide the dataset into two subsets, Dataset I and Dataset II. As summarized in Table 3, for Dataset 1 linear relations exist between $(\tau_2 - \tau_1)$ and $(\tau_1 - \bar{\tau})$ as well as between $(d_2 - d_1)$ and $(d_1 - \bar{d})$. Notably, all linear models are statistically significant at the 99% confidence level (p<0.01), with R^2 ranging from 0.43 to 0.84. Considering that individual driving behavior varies considerably, these R^2 values are quite reasonable, especially for d.

Table 3 Summary of modelling results using Dataset I (Sample size: 244)

Dependent Variable	Coefficient		p value	Overall Goodness of Fit	
				p value	R^2
$\tau_2 - \tau_1$	β	0.0934	0.38	<.01	0.43
	α	-0.526	<.01		
$d_2 - d_1$	β	3.235	0.06	<.01	0.84
	α	-0.883	<.01		

As in Zheng et al. (2011b), Equation (5) can be rearranged to

$$\tau_2 - \bar{\tau} = (\alpha + 1)(\tau_1 - \bar{\tau}) + \beta. \qquad (6)$$

Based on the results in Table 3, $-1 < \alpha < 0$ (or $0 < \alpha+1 < 1$) and $\beta \approx 0$, which indicates that the deviation of τ (or d) from the average driving behavior becomes smaller after crossing a deceleration wave because $0 < \alpha+1 < 1$. This

relationship implies that a timid driver, who is characterized by $\tau_1 - \bar{\tau} > 0$, becomes less timid after experiencing a deceleration wave, though the driver remains timid because $\tau_2 - \bar{\tau} > 0$. The same results are obtained using d. Thus, the model results suggest that a deceleration wave of an oscillation has a regressive effect on the driver's behavior by encouraging a timid (aggressive) driver to become less timid (aggressive), resulting in a change in deceleration duration of an oscillation.

For verification, we estimate linear models using Dataset II (see Table 4 for the results) and compare the results to those based on Dataset I in Table 3. The coefficients estimated using the two datasets are similar, though a larger difference is observed for $\tau_1 - \bar{\tau}$. All models based on Dataset II are also significant at the 99%, with R^2 ranging from 0.49 to 0.75. Note that the β term for $d_2 - d_1$ is statistically significant. However, the value is small relative to the range of d (-200-400 ft). Notably, the estimated coefficients in Tables 3 and 4 are comparable to the estimated coefficients of the same modelling framework in Zheng et al. (2011b); coefficients of $\tau_1 - \bar{\tau}$ range from -0.780 to -0.670, and coefficients of $d_1 - \bar{d}$ ranges from -0.819 to -0.778 in that paper. This indicates that the regressive effect can be instigated by different types of disturbances and that a driver changes her behavior in a similar manner regardless of the cause.

Table 4 Summary of modelling results using Dataset II (Sample size: 245)

Dependent Variable	Coefficient		*p* value	Overall Goodness of Fit	
				p value	R^2
$\tau_2 - \tau_1$	β	-0.0494	0.62	<.01	0.49
	α	-0.780	<.01		
$d_2 - d_1$	β	5.488	<.01	<.01	0.75
	α	-0.828	<.01		

It is possible that the change may not necessarily be a long-term behavioral change. We could not investigate this because the study sites were not long enough. Nevertheless, our results suggest that parameters τ and d for a driver are not fixed but time-dependent, especially around major disturbances like oscillations. This might be able to explain the spatial growth of disturbances, as recently theorized by Laval and Leclercq (2010).

Finally, we cross-validate the models; i.e., the models based on one dataset are used to predict τ_2 and d_2 in the other dataset. Figure 9(a) shows the prediction error in τ_2, which is calibrated using Dataset I and applied to Dataset II; approximately 60% of the predictions are within 0.8 sec (about 40% error). The validation result in Figure 9(b) with the calibration and validation datasets switched shows a similar trend. A similar conclusion can be reached for d_2, as shown in Figure 10. The validation results indicate that significant prediction errors exist, though the performance is reasonable given the simplicity of the model and large variations in driving behavior. Efforts to further improve the model's performance are ongoing. However, it might be more advantageous to use this simple model for more straightforward calibrations and better transferability since a complex model may increase the risk of over-fitting the data.

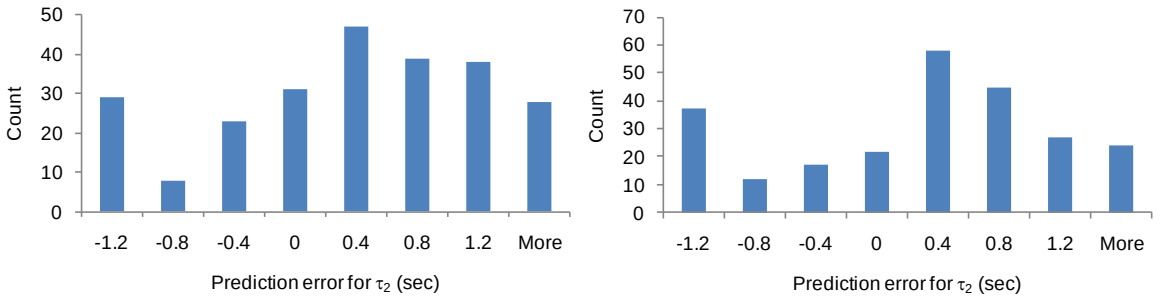

(a) (b)

Figure 9 Frequency distributions of prediction error in τ_2: (a) τ_2 calibrated using Dataset I and applied to Dataset II; (b) τ_2 calibrated using Dataset II and applied to Dataset I.

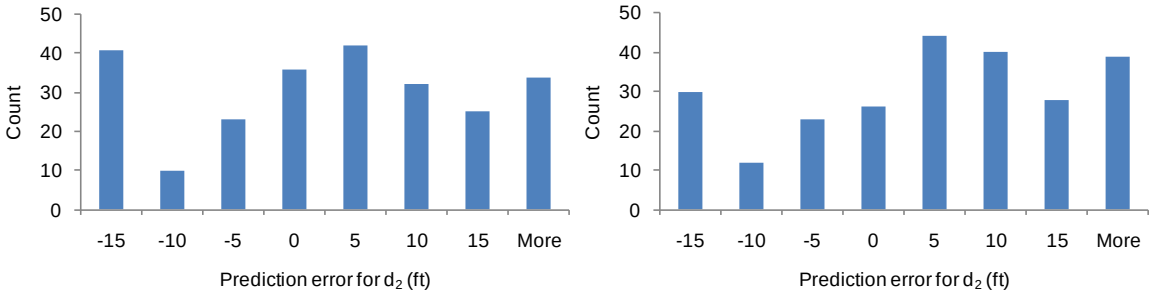

Figure 10 Frequency distributions of prediction error in d_2: (a) d_2 calibrated using Dataset I and applied to Dataset II; (b) d_2 calibrated using Dataset II and applied to Dataset I.

6. Conclusions

In this paper, we adopted the WT method to systematically analyze oscillations' origins and measure their propagation characteristics (i.e., propagation speed, duration, amplitude, and intensity) using vehicle trajectory data. The results from 53 oscillation cases show that traffic oscillations can be triggered by either LCMs or instabilities in driver CF behavior. However, the primary trigger was site-specific. Most oscillations were triggered by LCMs on I-80, where no particular horizontal and vertical alignments were present. In contrast, a larger proportion of oscillations (~65%) formed spontaneously without LCMs on US-101, probably caused by rubbernecking due to the presence of workers on the side of the road.

The analysis results also suggest that propagation features are similar between cases regardless of the trigger. All 53 cases exhibited a precursor phase, in which oscillations were isolated at a nearly fixed location, and 22 eventually emerged from the precursor phase and propagated upstream with increased amplitudes. LCMs were primarily responsible for this transition into the well-developed phase (15 out of 22 cases), although some transitions did occur without LCMs (7 cases).

Finally, we found some evidence suggesting that driver behavior may be different before and after the oscillation. A simple statistical model suggests that 1) the changes in τ or d are linearly related to the deviations from the average driving behavior (represented by average τ and d); 2) a timid (aggressive) driver with larger (smaller) response time and/or minimum spacing becomes less timid (aggressive) after experiencing a deceleration wave; and 3) an oscillation is unlikely to convert a timid driver to an aggressive one or vice versa. These findings are similar to those reported in Zheng et al. (2011b) with the exception that the regressive effect was induced by LCMs in that study. Thus, our findings imply that a driver corrects herself to drive more "normally" after experiencing a major disturbance regardless of the type of disturbance. This controversial finding, however, may be due to the limited spatial extent of trajectories, which might have precluded us from observing the full recovery after the oscillation. Nevertheless, our findings indicate that parameters τ and d are time-dependent unlike the premise of Newell (2002).

References

Addison, P.S. (2002). *The illustrated wavelet transform handbook: Introductory theory and applications in science, engineering, medicine and finance*, Taylor & Francis.

Ahn, S. & Cassidy, M.J. (2007). Freeway traffic oscillations and vehicle lane-change maneuvers. *Proceedings of the 17Th International Symposium on Transportation and Traffic Theory*, Amsterdam, Elsevier, 691-710.

Ahn, S., Laval, J.A., & Cassidy, M.J. (2010). Merging and diverging effects on freeway traffic oscillations: theory and observations. *Transportation Research Record, Journal of the Transportation Research Board*, 2188, 1-8.

Ahn, S. (2005). *Formation and spatial evolution of traffic oscillations*. Doctoral Dissertation, Department of Civil and Environment Engineering, University of California, Berkeley.

Ahn, S., Cassidy, M.J., & Laval, J.A. (2004). Verification of simplified car-following theory. *Transportation Research Part B*, 38(5), 431-440.

Del Castillo, J.M. (2001). Propagation of perturbations in dense traffic flow: A model and its implications. *Transportation Research Part B*, 35(4), 367-389.

Donoho, D.L. (1993). Unconditional bases are optimal bases for data compression and for statistical estimation. *Applied and Computational Harmonic Analysis* 1(1), 100-115.

Edie, L.C., & Baverez, E. (1965). Generation and propagation of stop-start traffic waves. Vehicular Traffic Science, *Proceedings of the 3rd International Symposium on the Theory of Traffic Flow*, New York, 26-37.

FHWA. The next generation simulation (NGSIM). <http://www.ngsim.fhwa.dot.gov/> (05/08, 2008).

Fugal, D. (2009). *Conceptual wavelets in digital signal processing: an in-depth, practical approach for the non-mathematician*. Space and Signals Technical Publishing.

Herman, R., Montroll, E.W., Potts, R.B., & Rothery, R.W. (1959). Traffic dynamics: analysis of stability in car following. *Operations Research*, 7, 86-106.

Kerner, B., & Rehborn, H. (1996). Experimental features and characteristics of traffic jams. *Physical Review E*, 53(2), 1297-1300.

Kim, T., & Zhang, H. (2008). A stochastic wave propagation model. *Transportation Research Part B*, 42(7-8), 619-634.

Laval, J.A., & Leclercq, L. (2010). A mechanism to describe the formation and propagation of stop-and-go waves in congested freeway traffic. *Philosophical Transactions of The Royal Society A: Mathematical Physical and Engineering Sciences*, 368, 4519-4541.

Li, X., Peng, F., & Ouyang, Y. (2010). Measurement and estimation of traffic oscillation properties. *Transportation Research Part B*, 44(1), 1-14.

Lighthill, M., & Whitham, G. (1955). On kinematic waves: II. A theory of traffic flow on long crowded roads. *Proceedings of the Royal Society of London. Series A, Mathematical and Physical Sciences*, 229(1178), 317-345.

Lu, X. & Skabardonis, A. (2007). Freeway traffic shockwave analysis: Exploring the NGSIM trajectory data, *Proceedings of the 86th TRB Annual Meeting*, Washington D.C., January 2007, TRB Paper #07-3016, CD-ROM.

Ma, T., & Ahn, S. (2008). Comparisons of speed-spacing relations under general car following versus lane changing. *Transportation Research Record, Journal of the Transportation Research Board*, 2088, 138-147.

Mallat, S.G. (2009). *A wavelet tour of signal processing (Third edition): The sparse way*. Academic Press.

Mauch, M., & Cassidy, M.J. (2002). Freeway traffic oscillations: Observations and predictions. *Proceedings of the 15th International Symposium on Transportation and Traffic Theory*, Pergamon-Elsevier, Oxford, UK, 653–674.

Newell, G.F. (1993). A simplified theory of kinematic waves in highway traffic, part I: General theory. *Transportation Research Part B*, 27(4), 281-287.

Newell, G.F. (2002). A simplified car following theory: A lower order model. *Transportation Research Part B*, 36(3), 195-205.

Orosz, G., Wilson, R.E., Szalai, R., & Stépán, G. (2009). Exciting traffic jams: Nonlinear phenomena behind traffic jam formation on highways. *Physical Review E*, 80(4): 046205.

Richards, P.I. (1956). Shock waves on the highway. *Operations Research*, 4(1), 42-51.

Schoenhof, M., & Helbing, D. (2007). Empirical features of congested traffic states and their implications for traffic modeling. *Transportation Science*, 41(2), 135-166.

Smilowitz, K., Daganzo, C.F., Cassidy, M.J., & Bertini, R.L. (1999). Some observations of highway traffic in long queues, *Transportation Research Record*, 1678, 225-233.

Sugiyama, Y., Nakayama, A., Fukui, M., Hasebe, K., Kikuchi, M., Nishinari, K., Tadaki, S. & Yukawa, S. (2003). Observation, theory and experiment for freeway traffic as physics of many-body system, In M. Schreckenberg P. Bovy, S. Hoogendoorn and D.E. Wolf, editors, *Traffic and granular flow '03*, 45-59

Thiemann, C., Treiber, M., & Kesting, A. (2008). Estimating acceleration and lane-changing dynamics based on NGSIM trajectory data. *Transportation Research Record: Journal of the Transportation Research Board*, 2088, 90-101.

Wilson, R.E. (2008). Mechanisms for spatio-temporal pattern formation in highway traffic models. *Philosophical Transactions of The Royal Society A: Mathematical Physical and Engineering Sciences*, 366(1872), 2017-2032.

Yeo, H., & Skabardonis, A. (2009). Understanding stop-and-go traffic in view of asymmetric traffic theory. *Proceedings of the 18th International Symposium on Transportation and Traffic Theory*. Hong Kong, Springer, 99-116.

Zheng, Z., Ahn, S. & Monsere, C.M. (2010). Impact of traffic oscillations on freeway crash occurrences. *Accident Analysis and Prevention*, 42(2), 626-636.

Zheng, Z., Ahn, S., Chen, D., & Laval, J.A., (2011a). Applications of wavelet transform for analysis of freeway traffic: Bottlenecks, transient traffic, and traffic oscillations, *Transportation Research Part B*, 45(2), 372-384.

Zheng, Z., Ahn, S., Chen, D., & Laval, J.A., (2011b). The impact of lane-changing on the immediate follower: Anticipation, relaxation, and behavioral change, *Submitted.*